Noradrenergic plasticity of olfactory sensory neuron inputs to the main olfactory bulb.

Eckmeier D and Shea SD,

Cold Spring Harbor Laboratory, 1 Bungtown Road, Cold Spring Harbor, NY 11724, USA

Abstract

Sensory responses are modulated throughout the nervous system by internal factors including attention, experience, and brain state. This is partly due to fluctuations in neuromodulatory input from regions such as the noradrenergic locus coeruleus (LC) in the brainstem. LC activity changes with arousal and modulates sensory processing, cognition and memory. The main olfactory bulb (MOB) is richly targeted by LC fibers and noradrenaline profoundly influences MOB circuitry and odor-guided behavior. Noradrenaline-dependent plasticity affects the output of the MOB. However, it is unclear whether noradrenergic plasticity includes modulation in the glomerular layer, the site of input to the MOB. Noradrenergic terminals are found in the glomerular layer, but noradrenaline receptor activation does not seem to acutely modulate olfactory sensory neuron terminals *in vitro*. We investigated whether noradrenaline induces plasticity at the glomerulus. We used wide-field optical imaging to measure changes in odor responses following electrical stimulation of locus coeruleus in anesthetized mice. Surprisingly, the odor-evoked intrinsic optical signals at the glomerulus were persistently weakened after LC activation. Calcium imaging selectively from olfactory sensory neurons confirmed that this effect was due to suppression of presynaptic input. Finally, noradrenaline antagonists prevented glomerular suppression. We conclude that noradrenaline release from LC has long-term effects on odor processing already at the first synapse of the main olfactory system. This mechanism could contribute to arousal-dependent memories.

Keywords: olfactory bulb, neuromodulation, memory, noradrenalin, glomerulus, plasticity

Introduction

Neuronal firing patterns are continuously influenced by neuromodulators such as noradrenaline. Noradrenaline is released throughout the forebrain by the brainstem nucleus locus coeruleus (LC) and modulates sensory responses, cognition and behavior with arousal (reviewed in: Usher et al., 1999; Aston-Jones and Cohen, 2005; Bouret and Sara, 2005; Valentino and Van Bockstaele, 2008; Berridge et al., 2012; Devore and Linster, 2012). In the main olfactory bulb (MOB), noradrenaline is essential for certain forms of odor learning and discrimination, including learning of social odors (Pissonnier et al., 1985; Sullivan et al., 1989, 1992, 2000; Kendrick et al., 1991; Rangel and Leon, 1995; Brennan et al., 1998; Guérin et al., 2008; Mandairon et al., 2008). Nonetheless, the specific synaptic targets of long-term modulation by noradrenaline in the MOB remain unclear.

Olfactory sensory neurons (OSNs) make synapses onto mitral/tufted cells which project to deeper brain areas. OSN terminals and the apical dendrites of mitral/tufted cells form spherical glomeruli at the surface of the MOB (Chen and Shepherd, 2005). The glomeruli therefore constitute the first synapse in the main olfactory system. Because the glomeruli gather inputs from OSNs expressing the same receptor protein, they form functional units of spatial representations for odors (Mombaerts, 2006) that may be readily imaged (Rubin and Katz, 1999; Uchida et al., 2000; Meister and Bonhoeffer, 2001; Wachowiak and Cohen, 2001; Bozza et al., 2004; Lin et al., 2006; Fletcher et al., 2009; Ma et al., 2012). Deep to the glomeruli, the mitral/tufted cells receive inhibitory feedback from granule cells via dendrodendritic synapses onto their lateral dendrites (Jahr and Nicoll, 1980; Isaacson and Strowbridge, 1998).

Noradrenaline has both short-term and long-term effects on MOB activity. Granule cells are inhibited by α_1 adrenergic receptor agonists at some concentrations (Nai et al., 2009, 2010; Linster et al., 2011). Mitral/tufted cells are also directly excited by noradrenaline (Hayar et al., 2001; Pandipati et al., 2010). These excitatory and disinhibitory effects may synergize to increase sensitivity to input (Jiang et al., 1996; Ciombor et al., 1999). It is suggested that transient

disinhibition of mitral/tufted cells leads to longer-term physiological changes in the MOB network (Pandipati et al., 2010). For instance, the mitral/tufted cells gradually habituate to an odor presented during noradrenaline release and the response remains suppressed afterwards (Wilson et al., 1987; Sullivan et al., 1989; Shea et al., 2008). This is correlated with a broad increase in levels of GABA relative to glutamate (Kendrick et al., 1992; Brennan et al., 1998) suggesting habituation involves active inhibition.

The circuit nodes affected by this enhanced inhibition remain uncertain. Noradrenaline modulates granule cell activity (Nai et al., 2009, 2010; Linster et al., 2011), and noradrenergic terminals from LC heavily target the granule cells (McLean et al., 1989; Winzer-Serhan et al., 1996, 1997; Day et al., 1997). However, noradrenergic terminals are found throughout the MOB and cells in the glomerular layer express adrenergic receptors (Winzer-Serhan et al., 1996, 1997; Day et al., 1997). These diverse interneurons (many of which are GABAergic) are positioned to regulate synaptic input from OSNs. Activation of noradrenaline receptors failed to acutely modulate signaling from OSNs, but long-term effects were not assessed (Hayar et al., 2001).

We investigated whether long-term modulation of the OSN input to the MOB is induced by electrical LC stimulation during odor presentation in anesthetized mice. We measured the activation of glomeruli with wide-field imaging of intrinsic optical and fluorescent calcium signals at the glomerular layer in the MOB. Surprisingly, after LC stimulation we observed a long-term reduction in signals from the OSNs. This effect was prevented by adrenergic receptor antagonists. Thus, arousal-dependent olfactory memories may alter odor-evoked synaptic activity as early as the first synapse in the main olfactory system.

Methods

Animals: Mice were 6-16 weeks old, of both sexes, and housed in the institution's animal facilities. Intrinsic optical signals were measured in C57/BL6 mice (Jackson Labs) and fluorescent calcium signals were measured in a transgenic mouse line (tetO-GCaMP2/OMP-IRES-tTA). To generate these mice, a tetO-GCaMP2 mouse line was crossed with another line carrying an OMP-IRES-tTA allele (He et al., 2008; Ma et al., 2012). In this mouse, expression of *OMP* leads to the transcription of a bicistronic RNA for both OMP and tTA (Yu et al., 2004) and in turn to expression of the fluorescent Ca^{2+} sensor GCaMP2 in olfactory sensory neurons.

Genotyping (tetO-GCaMP2/OMP-IRES-tTA): After weaning (d21) tail samples were collected form isofluorane-anaesthetized mice. The samples were solved in lysis buffer (10 mM NaOH and 0.1 mM EDTA) and additional proteinase K at 37°C. The proteinase K was deactivated in a 95°C water bath. The PCR solution included 1 µl of the DNA solution (diluted 20X), 10 µl PCR master mix (Promega GoTaq® Green Master Mix M7123), 7 µl nuclease free water and 1 µl of each primer (10µM; IDENTIFY 5' and 3' primers ATCGATTCTAGAATTCGCTGTCTG; CTTATCGTCATCGTCGTACAGAT). PCR cycle: 2 min at 95°C, 35 cycles (30s at 95°C, 1 min 53°C to 59°C, 1 min at 72°C), 5 min at 72°C, stored at 4°C.

Anesthesia: During all surgeries the mice were initially anaesthetized with ketamine and xylazine (100/5 mg/kg). The anesthesia was maintained with a syringe pump (Harvard Apparatus, Pump 11) loaded with a ketamine/saline solution (i.p. infusion; 90 mg/kg/h).

Implantation of the Stimulation Electrode: Tungsten electrodes (MicroProbes™; 1MΩ) were shortened to 8 mm from the tip and soldered to new contacts before implantation. Impedence measurement ensured that the electrodes were not damaged. During the procedure the location of the electrode tip was verified through electrophysiology. Locus coeruleus neurons exhibit a characteristic shape and rate of action potentials, and respond to tail pinches (Shea et al., 2008). The electrode was secured with dental cement and the scalp was sutured. The cut was further sealed with tissue adhesive (Vetbond™; n-butyl cyanoacrylate). An anti-inflammatory drug (Meloxicam or Loxicom) was injected to facilitate recovery (1-10 days, 1 mg/kg).

Acute Cranial Window: A cranial window for imaging was acutely implanted over the MOB immediately before the experiment. A plate with a round window was glued to the exposed skull over the main olfactory bulbs using Super Glue® (cyanoacrylate). After the glue had hardened, the mouse was placed in a warming tube and the head was fixed in a holder via the plate. A craniotomy was opened to reveal the dorsal surfaces of both main olfactory bulbs (compare figures 1 A and 3 A) using a dental drill and a breakable blade holder. Care was taken to remove the bone without injuring the dura mater. The craniotomy was filled with 1.5% agarose and covered with a round (3 mm diameter) cover glass that fits inside the window in the plate. For antagonist experiments, phentolamine (10 µM) and propranolol (10 µM) were dissolved in the agarose used to fill the imaging window. We tested the efficacy of this application method with gabazine and CNQX (see results).

Imaging Apparatus: The mouse was positioned under a CCD video camera (Vosskühler CCD-1300QF) attached to a macro-lens assembly (Nikon normal AF Nikkor 50 mm auto lens and Nikon telephoto AF DC Nikkor 105 mm lens) (Petzold et al., 2008). The camera was focused on the glomerular layer of the main olfactory bulbs. The aperture was set to 8 for intrinsic optical signals and 2 for fluorescent signals, the focal length was set to infinite. Light emitting diodes (LEDs) of different wavelengths were used for illumination. Intrinsic signals were visible in far/infrared light (~780 nm), while fluorescence was excited by blue light (470 nm wavelength). A band-pass emission filter was placed in front of the blue LEDs and a 510 nm long-pass optical filter (Chroma Filters HQ510lp) was placed in front of the CCD camera to filter out the blue light from the LED.

Odor Presentation: The odors were presented using a custom-built olfactometer containing an 8-way solenoid that controls oxygen flow through 8 vials, 7 of which contained odorants dissolved in mineral oil (0.5% or 1%), the remaining vial was empty (blank). Odorized

oxygen was diluted 5:1 into a continuous carrier stream for a total flow of 2.5 l/min. To prevent odor accumulation, air was collected behind the animal with a vacuum pump. Odor presentation was 20 s when measuring intrinsic signals and 3 s when measuring calcium signals.

Electrical Stimulation of Locus Coeruleus: The implanted electrode was connected to an isolated pulse stimulator (A-M Systems Model 2100) and a ground electrode was positioned under the skin behind the mouse's ear. The pulse generator was triggered 1 s prior to odor presentation onset. The stimulation consisted of 40 µA biphasic pulses of 100 µs duration generated at 5 Hz for 24 s (intrinsic optical imaging) or 5 s (calcium imaging).

Automated Experimental Control and Data Acquisition: Custom software written in LabView (written by DE) controlled the data acquisition hardware and stimulus delivery according to a scripted protocol. The olfactometer, LEDs, and pulse stimulator were controlled by a digital I/O card (National Instruments, PCI-6503) connected with the devices via a terminal block (National Instruments, CB-50LP). For camera control and image acquisition a separate image acquisition card (National Instruments IMAQ PCI-1422-LVDS).

Imaging Protocol: During each trial, images were acquired from the camera before, during and after odor presentation and stored as monochromatic image stacks. For intrinsic signals we acquired 250 frames before, 500 frames during and another 250 frames after odor presentation at 25 frames per second (fps). For fluorescent signals we acquired 100 frames before, 75 frames during and 50 frames after odor presentation at 25 frames per second (fps). Differences in the frame counts for the two measurements reflect the different time scales necessary to acquire reliable signals.

Experimental Sequence: First, 7 different odors and clean air were each presented three times in a 'pretest'. Based on the responses, two odors were selected for the experiment. The two odors were presented alternately throughout the experiment. Experiments had a pairing phase of 30 repetitions during which both odors were presented and one of which was paired with locus coeruleus stimulation. Imaging phases span 15 – 20 repetitions and occurred before and after the pairing phase.

Verification of the Stimulation Site: After the experiment ended, the position of the stimulation electrode was marked by an electrolytic lesion using a pulse stimulator (three pulses at -10 µA, 10 s). Then the mouse was given a lethal injection of Euthasol and perfused with PBS followed by 4% paraformaldehyde. The skull was stored in paraformaldehyde overnight before the brain was extracted. The brain was then placed in 30% sucrose in PBS overnight, cut into 60 µm slices and stained with cresyl violet.

Data analysis: For quantification, the raw image stacks were analyzed with our custom Matlab (Mathworks) software (written by DE). Active areas on the olfactory bulb were made visible by dividing the average frame image acquired during stimulation by the average frame image acquired prior to stimulation (Meister and Bonhoeffer, 2001). Typical results are shown in figures 1 C and 3 C. Regions of interest that corresponded to activated glomeruli for each odor were identified and the mean grayscale value was computed frame-by-frame from the raw image data. This produced a signal trace for every repetition and every glomerulus. The single repetition traces were then averaged for repetitions before and after odor pairing, respectively (blue traces in figures 1 D and 3D). Low frequency baseline shifts were corrected by fitting an exponential function to the baseline (dotted lines in figures 1 D and 3D) and subtracting it from the data (red traces in figures 1 D and 3D). Only glomeruli that showed a clear response correlated with odor onset in at least one of the experimental phases were included in the study. From the traces we calculated the signal strength for each experimental phase as $(|R_b-R_a|)/R_b*100$ with R_b being the mean baseline reflectance/fluorescence and R_a the mean reflectance/fluorescence during odor stimulation (plateau phase).

Statistics: The Kruskal-Wallis test (a test for difference of independent, non-parametric distributions) followed by Tukey's honestly significant difference test was used to identify statistically significant differences (Matlab, Mathworks).

Results.

We aimed to assess the long-term effects of noradrenaline from LC on odor responses in the glomeruli. We chose to use wide-field imaging because it allowed us to measure the amplitude of glomerular signals over an extended time period for multiple glomeruli (Rubin and Katz, 1999; Uchida et al., 2000; Meister and Bonhoeffer, 2001; Wachowiak and Cohen, 2001; Bozza et al., 2004; Lin et al., 2006; Fletcher et al., 2009; Ma et al., 2012). As an initial step, we imaged intrinsic optical signals (IOS), which reveal spots of activity that correspond to glomeruli.

IOS reveal odor-activated glomeruli at the dorsal surface of the main olfactory bulbs

To illustrate the signals we acquired, we show examples of IOS imaging data in Figure 1. Figure 1A is an average video frame. The red and blue circles indicate where we found activated glomeruli in the activation patterns elicited by two different odors. The red and blue arrows were introduced as landmarks that reappear in figure 1B. Each panel in figure 1B shows the activation pattern by one odor on the left main olfactory bulb. The glomeruli are visible as round black spots. The left panel depicts the activation pattern that is marked in blue in figure 1A; the right panel depicts the glomeruli marked in red in figure 1A. The images are baseline-subtracted averages of the images collected during odor presentation. We further applied a high-pass filter to remove the low frequency components of the signal that are unrelated to the glomerular activity (Meister and Bonhoeffer, 2001).

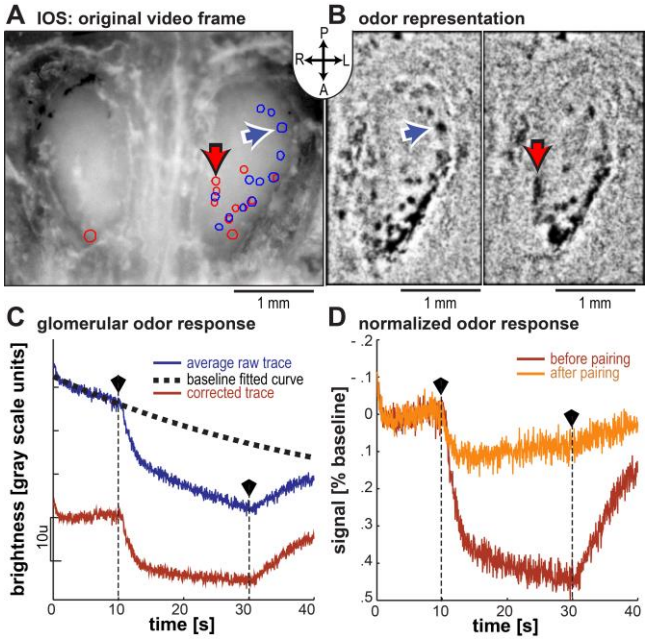

Figure 1 Intrinsic signals revealed the odor representation at the level of glomeruli. Panel A shows an image of the dorsal surfaces of the main olfactory bulbs acquired during IOS imaging. Both hemispheres were included, with the rostral pole facing down (inset: A-anterior, P-posterior, L-left, R-right). Blue and red circles indicate the active areas for the two presented odors. Red and blue arrows point to one glomerulus of each representation to allow comparison with B. B shows the representation of each odor on the left hemisphere. The blue and red arrows point at the same glomeruli as in A. These images were generated by subtracting images acquired during odor presentation from those acquired prior to odor presentation. C shows a trace of grayscale values in one glomerulus. The trace was averaged over 20 repetitions. The original trace (blue curve) showed an artificial slow decay that was corrected by fitting an exponential function (dotted curve) which was then subtracted from the original trace (red curve). The polygonal black markers and vertical dotted lines mark beginning and end of odor presentation. In D we show the corrected signals from C (red curve), which were acquired prior to pairing the odor with locus coeruleus stimulation. They are contrasted with the signal averaged across 20 repetitions that were acquired after the pairing phase (orange curve). The curves were normalized to the baseline average (prior to odor onset). Y axes therefore indicate the deviation from baseline activation in percent of the baseline. We inverted the Y axis so that higher values indicate stronger activation.

The temporal structure of the odor response is shown in figure 1C. The blue line shows the mean gray scale value within one of the identified glomeruli for each frame of the raw image stack, averaged over the first twenty repetitions of the same odor. There is a clear deflection of the signal in response to odor onset at 10 s. The odor delivery was turned off after 20 s and the signal recovered. This signal was embedded in a slowly decaying baseline that resulted from instability in the

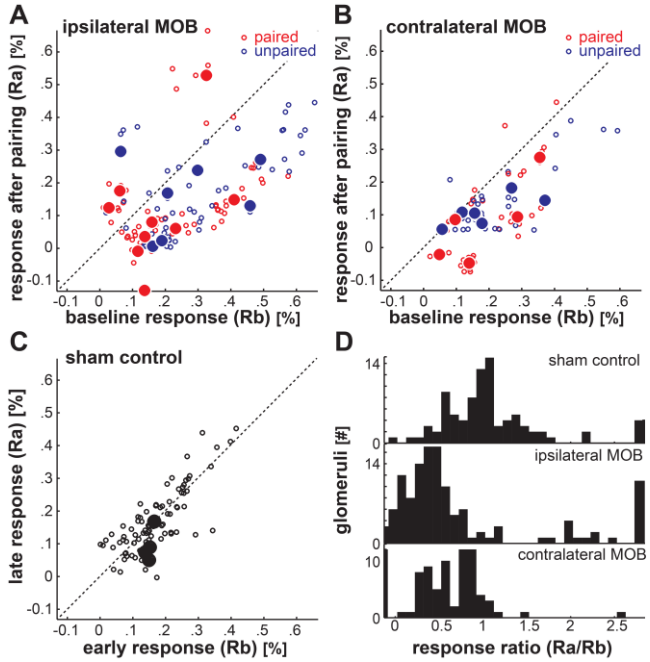

Figure 2 Intrinsic optical signals indicate a habituation of glomerular responses after a period of pairing odor presentation with locus coeruleus stimulation. In panels A-C the Y axis indicates response strength after pairing while the X axis indicates response strength before pairing. Small circles indicate the activation of glomeruli, large filled circles indicate the median for each animal and odor. A and B show the data for glomeruli responding to the paired odor (red) and unpaired odor (blue) on the hemisphere ipsilateral and contralateral to the stimulated locus coeruleus, respectively (9 animals). Panel C shows the results of the sham control (4 animals). Data from both odors and hemispheres were combined in this case. For D the ratio between the response before and after pairing was calculated for each odor. The histogram indicates the distribution of glomeruli for the sham control, and for the actual experiment divided by hemisphere.

illumination LEDs. We corrected for this artifact by fitting an exponential function to the pre-odor baseline (figure 1C, dotted line) and then subtracting it from the data (figure 1C, red line). Comparing the corrected mean response collected from one glomerulus before and after LC stimulation shows that the response strength (percent decrease from baseline; figure 1D) differs.

IOS are suppressed after pairing odors with LC stimulation.

We measured the effects of LC activation on intrinsic optical signals in the MOB. During the experiment, we paired the presentation of one of two odors with electrical stimulation of LC via an implanted electrode thirty times. Before and after stimulation we imaged the response of the glomeruli activated

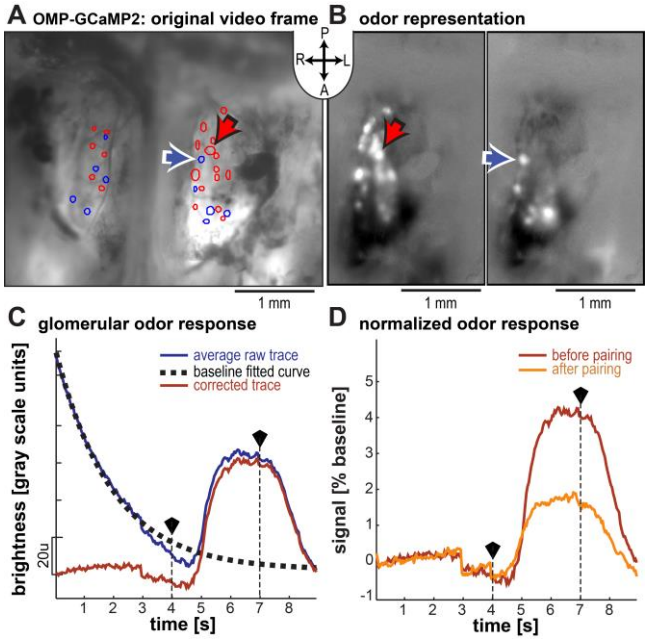

Figure 3 Fluorescent OSN calcium signals revealed the odor representation at the level of glomeruli. Panel A shows an image of the dorsal surfaces of the main olfactory bulbs acquired during fluorescence imaging. Both hemispheres were included, with the rostral pole facing down (inset: A-anterior, P-posterior, L-left, R-right). Blue and red circles indicate the active areas for the two presented odors. Red and blue arrows point to one glomerulus of each representation to allow comparison with B. B shows the representation of each odor on the left hemisphere. The blue and red arrows point at the same glomeruli as in A. These images were generated by subtracting images acquired during odor presentation from those acquired prior to odor presentation. C shows a trace of grayscale values in one glomerulus. The trace was averaged over 20 repetitions. The original trace (blue curve) showed an artificial slow decay that was corrected by fitting an exponential function (dotted curve) which was then subtracted from the original trace (red curve). The polygonal black markers and vertical dotted lines mark beginning and end of odor presentation. In D we show the corrected signals from C (red curve), which were acquired prior to pairing the odor with locus coeruleus stimulation. They are contrasted with the signal averaged across 20 repetitions that were acquired after the pairing phase (orange curve). The curves were normalized to the baseline average (prior to odor onset). Y axes therefore indicate the deviation from baseline activation in percent of the baseline.

by both odors for 20 trials each. Control mice were treated identically, but we did not apply a stimulation current to LC.

In mice that received no stimulation current in LC, the glomerular IOS measured before and after LC stimulation were indistinguishable. In figure 2C, the mean response strength for the last 20 trials is plotted over the mean response strength for the first 20 trials, for each glomerulus (n=88, from both hemispheres; n = 4 mice). The large markers indicate median values for each animal. Clustering of the data along

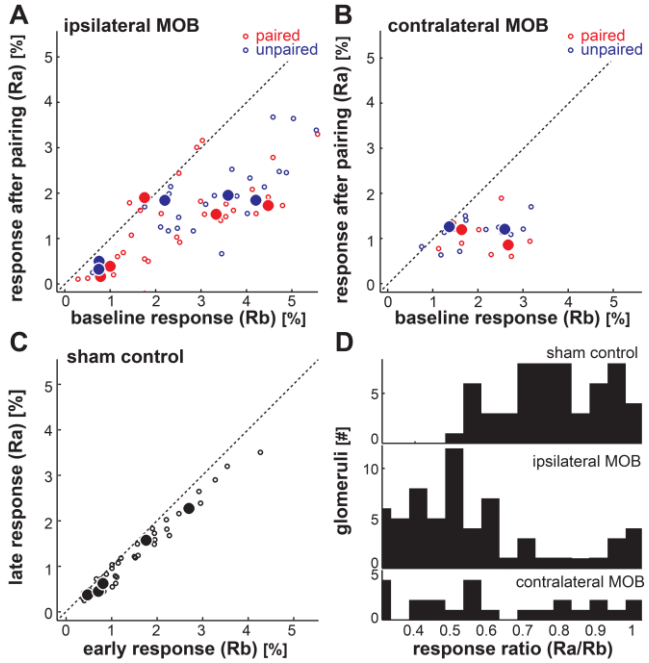

Figure 4 Fluorescent OSN calcium signals indicate a habituation of glomerular responses after a period of pairing odor presentation with locus coeruleus stimulation. In panels A-C the Y axis indicates response strength after pairing while the X axis indicates response strength before pairing. Small circles indicate the activation of glomeruli, large filled circles indicate the median for each animal and odor. A and B show the data for glomeruli responding to the paired odor (red) and unpaired odor (blue) on the hemisphere ipsilateral and contralateral to the stimulated locus coeruleus, respectively (5 animals). Panel C shows the results of the sham control (5 animals). Data from both odors and hemispheres were combined in this case. For D the ratio between the response before and after pairing was calculated for each odor. The histogram indicates the distribution of glomeruli for the sham control, and for the actual experiment divided by hemisphere.

the unity line demonstrates that response strengths were stable and unaffected by sham LC stimulation.

In contrast, in mice that did receive LC stimulation (paired), IOS signals in response to both odors were largely suppressed from baseline levels during the post-stimulation phase (Figure 2A, B). Most glomeruli on both hemispheres exhibited reduced responses after the pairing (n = 127 glomeruli, ipsilateral MOB; n = 82 glomeruli, contralateral MOB; n = 9 mice), as the data points are mostly below the unity line. Note that some glomeruli increased responses after the pairing, but all of them derived from one experiment. Figure 2D shows histograms of the ratio between the post-stimulation and baseline response strengths (suppression ratio, see Materials and Methods) for all glomeruli in control mice, ipsilateral glomeruli in paired mice, and contralateral glomeruli in paired mice. For both populations of glomeruli (ipsilateral and contralateral) in paired mice, this ratio was significantly lower

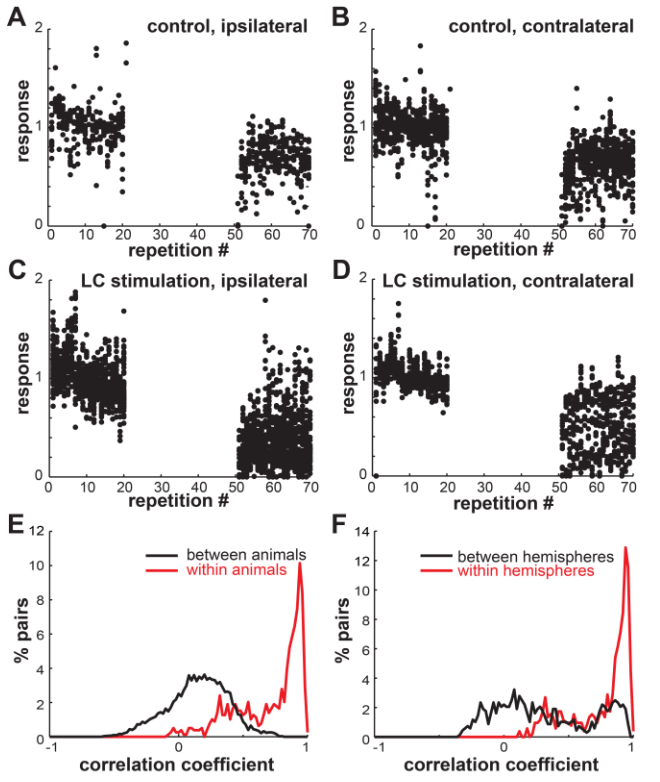

Figure 5 Trial by trial calcium signals and correlation between glomeruli. We show the calcium response of all glomeruli to the two odors on each hemisphere from all animals. All plots indicate the response strength during the experiment, normalized to the mean activation during the first 20 odor presentations, as the baseline varied for each glomerulus. No imaging was performed during the locus coeruleus activation. Panels A and B show for sham control experiments the responses of glomeruli on the hemispheres ipsi- and contralateral to the stimulation electrode, respectively. Panels C and D present the appropriate data for animals undergoing LC stimulation. Panels E and F present correlation histograms as percent pairs over correlation coefficient (bin size 0.04). Autocorrelations were omitted. In E the red line corresponds to pairs of glomeruli responding to the same odor in the same mouse. The black line shows correlation of glomeruli from different animals. In F the red line corresponds to pairs of glomeruli which respond to the same odor and are located in the same hemisphere. The black line corresponds to pairs of glomeruli which respond to the same odor but were found on different hemispheres of the MOB.

than 1 (for the non-normally distributed data we report the median and the upper bounds of the 1st and 3rd quartiles [Q_1 and Q_3 respectively]. ipsilateral: median: 0.44, Q_1: 0.25, Q_3: 0.76; contralateral: median: 0.58 , Q_1: 0.30, Q_3: 0.84 ; Wilcoxon signed rank test, contralateral: p = 0.000, ipsilateral: p=0.000), However this was not the case for glomeruli in control mice (median: 0.9975 , Q_1: 0.728, Q_3: 1.27 ; Wilcoxon signed rank test, p=0.89). Comparison of the three distributions showed that both paired distributions

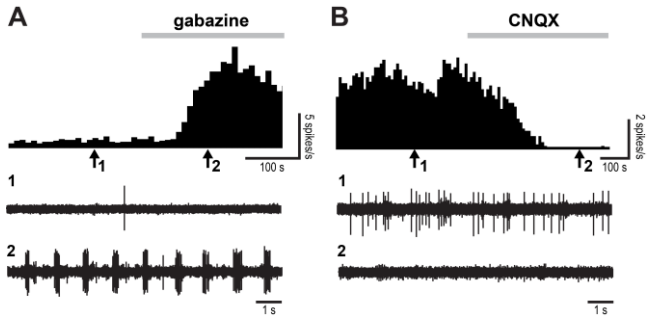

Figure 6 Application of drugs superficially in agarose effectively manipulates glomerular transmission. We dissolved gabazine (A) or CNQX (B) in agarose (10µM) and applied the agarose to the surface of the MOB. Mitral cell firing was measured with extracellular electrophysiology. Panels A and B: upper panel shows a histogram (bin size: 10s) of spike rates during application of gabazine (A) or CNQX (B). The gray bar indicates the application of drug. The middle (1) and bottom (2) panels show raw recording traces taken at time points corresponding with the arrows 1 and 2 respectively. Gabazine successfully disinhibited mitral cells and CNQX successfully inhibited mitral cell firing.

significantly differed from the control distribution (Kruskal-Wallis, $\chi^2 = 53.75$, p = 0.000, posthoc Tukey's HSD) but not from each other (posthoc Tukey's HSD).

Although only one of the odors was paired with LC stimulation, the suppression of glomerular responses was observed for both odors. Comparison between the distributions of suppression ratio for the paired odor and the unpaired odor yielded no significant difference (Kruskal-Wallis, $\chi^2 = 0.86$, p = 0.35). Thus, LC-mediated plasticity of glomerular responses is not odor specific for this simulation protocol.

Imaging fluorescent calcium signals in olfactory sensory neurons sensitively and selectively measures sensory input to the main olfactory bulb.

While intrinsic optical signals are closely correlated with the activity of OSNs, the extent of contributions from other glomerular elements to these signals remains unclear. We hypothesized that the changes we observed in glomerular activity after LC stimulation were due to reduced synaptic input from OSNs**.** Therefore, we moved on to more directly measure OSN synaptic input using wide-field fluorescence imaging in a mouse line that expresses the genetically encoded calcium sensor GCaMP2 exclusively in OSNs (OMP-GCaMP2) (Yu et al., 2004; He et al., 2008; Ma et al., 2012).

We treated raw data for GCaMP2 fluorescence signals from OSNs in the same manner as data from IOS experiments (Figure 3). Figure 3A is a video frame taken from one experiment. The red and blue circles indicate activated glomeruli that responded to two different odors. The red and blue arrows are landmarks for comparison with figure 3B, which shows two images of the left main olfactory bulb. The images were produced by subtracting the average baseline image from an average image taken during odor presentation. The round bright dots are glomeruli that were activated in response to the odor. The left image shows the glomerular activation pattern marked in red in figure 3A, the right one shows the glomerular activation pattern marked in blue in figure 3A.

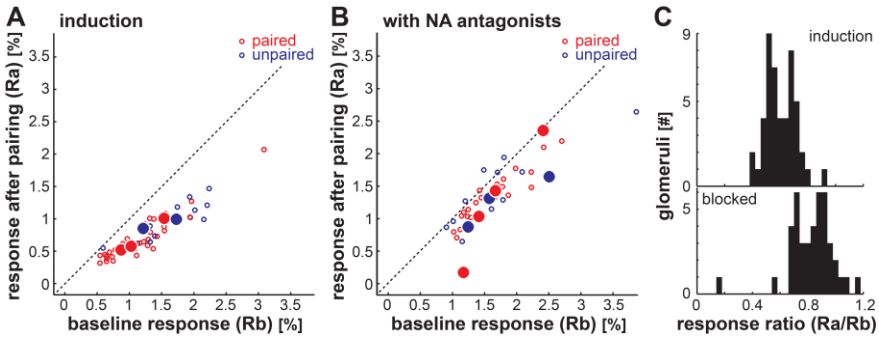

Figure 7 Blocking noradrenalin receptors abolished plasticity. In panels A-B the Y axis indicates response strength after pairing while the X axis indicates response strength before pairing. Small circles indicate the activation of glomeruli, large filled circles indicate the median for each animal and odor. A and B show glomeruli responding to the paired odor (red) and unpaired odor (blue) on both hemispheres, for the animals treated with noradrenalin antagonists (B, 4 animals) and untreated animals (A, 3 animals). For C the ratio between the response before and after pairing was calculated for the glomeruli in each group and the distribution is illustrated in the histogram.

As in the IOS data, responsive glomeruli identified in the differential images baseline subtracted images were selected for further analysis. The brightness of the glomerulus clearly increases just after odor onset (figure 3C, at 4s). Figure 3C is the average trace over twenty repetitions (blue line). The odor delivery lasted 3s and the signal subsequently returned to baseline. As with the IOS data, we corrected for slow baseline decay in brightness. Comparison of the mean baseline-corrected responses taken before and after the stimulation phase, respectively, reveals a clear suppression following the stimulation phase (Figure 3D). The response strength is expressed as percent increase from the baseline.

Fluorescent calcium signals in OSNs are suppressed after pairing odors with LC stimulation.

In these experiments, we measured the effects of LC stimulation specifically on the presynaptic input from OSNs in OMP-GCaMP2 mice. As before, we repeatedly paired the stimulation of LC with the presentation of one of two odors and imaged the response to both odors before and after this stimulation phase. Figure 4 depicts the results of these experiments in the identical format as in Figure 3. In the absence of LC stimulation (sham control experiment), the calcium signals from OSNs at the glomeruli did not change (n=58, from both hemispheres; n = 5 mice). This is illustrated by the scatter plot in figure 4C, in which the data for most glomeruli fall close to the unity line.

However as seen with IOS, the fluorescent calcium response to odors was suppressed after LC stimulation (Figure 4A,B). The measurements for nearly all glomeruli on both hemispheres (n = 62 glomeruli, ipsilateral MOB; n = 24 glomeruli, contralateral MOB; n = 5 mice) were at or below the unity line. Plotted as histograms of suppression ratio, the distributions for ipsilateral and contralateral glomeruli in paired mice were significantly lower than 1 (ipsilateral: median: 0.5, Q_1: 0.41, Q_3: 0.61; contralateral: median: 0.55, Q_1: 0.43, Q_3: 0.85; Wilcoxon signed rank test, contralateral: p = 0.000, ipsilateral: p=0.000). In contrast to the findings with IOS, the sham control mice also show a deviation from 1 which we attribute to bleaching (median: 0.78, Q_1: 0.67, Q_3: 0.90; Wilcoxon signed rank test, p=0.000). Comparison of the populations shows that the distributions of ipsilateral and contralateral glomeruli differ significantly from the distribution of control glomeruli (Kruskal-Wallis; χ^2 = 34.86; p = 0.001; posthoc Tukey's HSD), but not from each other.

As was the case with the IOS data, the suppression of glomerular responses was evident for both the paired and unpaired odors. Comparing the suppression ratios for glomeruli responsive to the paired and the unpaired odor, we found there was not a significant difference (Kruskal-Wallis; χ^2 = 3.02; p = 0.083). These data confirm that LC-mediated plasticity of OSN input to the glomeruli is not odor specific for this pairing regime.

Odor responses imaged in OMP-GCaMP2 mice were sufficiently strong and reliable to permit examination of the fluctuations of responses from trial to trial. In figure 5A-D we show the trial by trial data for these experiments. The scatter plots indicate the response strength of each glomerulus normalized to the baseline activity during each odor presentation. We did not image during the LC stimulation period (repetitions 21-50) to limit bleaching effects. A general downward shift is apparent, however, glomeruli which were activated during LC stimulation were further suppressed.

The change in signal strength over repetitions in glomeruli which respond to the same odor and are located on the same

hemisphere were highly correlated. To show correlations between groups of glomeruli we present correlation histograms as percent of pairs over the correlation coefficient (bin size = 0.04 bins) in figures 5E,F. In figure 5 E we show that glomeruli which respond to the same odor within a mouse correlate well (red line) while glomeruli do not correlate across animals (black line). In Figure 5 F we show that glomeruli which respond to the same odor but are localized on different hemispheres correlate only weakly (black line) while those which are located on the same hemisphere correlate well.

Effects of LC stimulation on OSNs depend on noradrenaline receptors.

Using two independent imaging methods we showed that LC stimulation triggers long-term changes in glomerular responses to odors, and we attribute these changes to reduced synaptic activity at OSN terminals. The question remains whether these effects are caused by noradrenaline release in the glomerular layer, or they involve an indirect mechanism. To answer this question, we topically applied the α- and β-noradrenergic receptor antagonists phentolamine and propranolol to the MOB surface during imaging experiments.

Drugs were dissolved in the agarose that was placed under the cranial window (see Materials and Methods). We performed electrophysiology control experiments with gabazine (10 µM; n = 2) and NBQX (10 µM; n = 2) to validate this delivery method. Gabazine and NBQX reliably and reversibly excited and suppressed activity respectively in the mitral cell layer (Figure 6) when dissolved in agarose and applied to the dorsal surface of the MOB. In pilot experiments, we observed that medium – high doses (> 60µM) of phentolamine and propranolol alone or in combination abolished odor responses (not shown). When we lowered the concentration to 10 µM, the odor responses remained stable throughout a timeframe suitable for our experiments. Given the low dose of antagonists, and in order to operate within the potentially limited window of drug effects, we chose to apply a moderated LC stimulation protocol as described by (Shea et al., 2008).

In the absence of antagonists, this LC stimulation regime reliably resulted in a suppression of fluorescent calcium signals after the stimulation phase (Figure 7A; n = 48 glomeruli; n = 3 mice). The magnitude of this suppression was significantly attenuated in the presence of phentolamine and propranolol (Figure 7B; n = 48 glomeruli; n = 3 mice). The histogram of suppression ratio in figure 7C reveals a rightward shift in the distribution with antagonists as compared to the distribution of glomeruli without antagonists. These two distributions were significantly different (Kruskal-Wallis, χ^2 = 43.66, p = 0.000). Thus, the observed suppression of OSN input to the MOB after LC stimulation at least partly depends on noradrenaline receptor activation in the superficial MOB.

Discussion.

Here we investigated noradrenergic modulation of synaptic input from olfactory sensory neurons to the glomeruli of the main olfactory bulb in anesthetized mice. By comparing the magnitude of IOS odor responses in the glomeruli before and after LC stimulation during odor exposure, we found that glomerular activity was suppressed long-term by noradrenaline. Subsequent imaging experiments using mice expressing the genetically-encoded calcium sensor GCaMP2 selectively in OSNs allowed us to confirm that this suppression includes modulation of presynaptic input to the glomeruli. Pharmacological manipulations revealed that LC-mediated suppression required noradrenergic receptor activation in the glomerular layer.

We were surprised to find that OSN terminals undergo long-term modulation by noradrenaline. Although noradrenergic fibers from LC course through all layers of the MOB (McLean et al., 1989), and noradrenergic receptors are present in the glomerular layer (Winzer-Serhan et al., 1996, 1997; Day et al., 1997), these inputs are sparser than those to deeper layers. Moreover, an *in vitro* study that examined modulation of signaling in the glomerulus did not detect any acute changes in the presence of noradrenaline (Hayar et al., 2001). Interestingly, odor conditioned fear memories were also recently shown to modify presynaptic glomerular inputs (Kass et al., 2013).

The role of granule cells in the noradrenergic modulation of mitral/tufted cells has been the subject of more intensive study than the glomerular processes. *In vitro* studies of the MOB circuit have established that noradrenaline acutely enhances the sensitivity of mitral/tufted cells to odor input directly and via release of inhibition from granule cells (Hayar et al., 2001; Nai et al., 2010; Pandipati et al., 2010; Linster et al., 2011). These *in vitro* observations are consistent with the acute effects of LC stimulation *in vivo* (Jiang et al., 1996). The synergy of sensitization and disinhibition of the mitral cells has been proposed as a key step in initiating long-term changes to the MOB network, including habituation or suppression of mitral/tufted cells and enhancement of oscillatory rhythms (Brennan and Keverne, 1997; Gire and Schoppa, 2008; Shea et al., 2008; Pandipati et al., 2010).

Shea et al (2008) also stimulated LC *in vivo* during odor presentation and found that odor responses in mitral/tufted cells were suppressed after LC-odor pairing. The effects we see on OSNs appear very similar. It seems likely that the reduced odor response in the mitral/tufted cells is, at least in part, a consequence of the effects we found in the olfactory sensory neurons. We also stimulated LC unilaterally; however

by imaging both olfactory bulbs we observed OSN input suppression in both hemispheres of the main olfactory bulb. This was not completely unexpected as it is known that a minority of noradrenergic LC neurons decussate and terminate in the contralateral MOB. Consistent with this asymmetry, the suppression in the contralateral hemisphere was smaller than in the ipsilateral hemisphere.

Our data contrast with the results of the previous study in mitral/tufted cells (Shea et al., 2008) in one important respect. Although we presented two odors during the pairing phase and paired only one of them with LC stimulation, significant suppression of glomerular responses was observed for both odors as compared to sham stimulation experiments. There was a tendency for the suppression of responses to the unpaired odor to be weaker than the suppression of responses to the paired odor in GCaMP2 imaging experiments using 20 s LC stimulation trains, however this difference was not statistically significant ($p = 0.083$). A weak bias such as this could conceivably be amplified among the mitral/tufted cells through additional modulation by granule cells.

How does plasticity of OSN input to the MOB occur? One possibility is that OSN synaptic terminals undergo enhanced inhibition from periglomerular cells. Periglomerular cells are GABAergic and regulate synaptic input to the glomeruli through presynaptic inhibition of OSN terminals (Murphy et al., 2005). These cells could therefore be a source for increased GABA release in response to a memorized odor that is observed *in vivo* after noradrenaline-dependent odor learning (Kendrick et al., 1992; Brennan et al., 1998). The periglomerular cells also make complex connections with other cell types in the glomerulus, therefore modulation of periglomerular cells would likely have consequences downstream from OSN input as well (Smith and Jahr, 2002; Schoppa and Urban, 2003; Murphy et al., 2005; Arruda et al., 2013).

At first, it may seem counterintuitive that sensory responses to a learned stimulus would be reduced rather than sensitized. However, habituation – diminishing behavioral responses to a repeated and therefore familiar stimulus – is one of the most fundamental forms of learning. Behavioral habituation is frequently manifested in the brain by neuronal habituation (Horn, 1986). Moreover, sensory plasticity frequently includes dynamic increases in inhibition (reviewed in: Carcea and Froemke, 2013). Broad inhibition is an important component for enhancing the salience or 'signal-to-noise ratio' by filtering redundant or overlapping portions of competing representations (Olshausen and Field, 2004; Assisi et al., 2007; Koulakov and Rinberg, 2011; Sachdev et al., 2012; King et al., 2013). We speculate that this may be the case here. Ultimately, 'sparsening' of the representation will entail increases in the activity of a small number of neurons in response to the learned stimulus against a background of global response reduction. This may be implemented as a two-stage process consisting of a nonselective subtraction and rectification step followed by multiplicative amplification. We speculate that noradrenergic modulation of the glomeruli may be a mechanism for implementing the first stage of representational sparsening.

Putting our findings into a behavioral context, several forms of noradrenaline-dependent memories are accompanied by physiological changes in the main olfactory bulbs (Wilson et al., 1987; Sullivan et al., 1989; Yuan et al., 2002). Furthermore, selective behavioral and physiological changes in response to an odor can be induced by increasing release of noradrenaline in the presence of that odor (Sullivan et al., 2000; Shea et al., 2008). This simulates what would occur during an episode of arousal. We therefore argue that there is strong evidence that LC-mediated plasticity in the olfactory bulb constitutes an important mechanism for arousal to facilitate odor memory formation. Surprisingly, these memories seem to affect even the initial detection of a stimulus by altering the signal as early as in the receptor neurons.

References.

Arruda D, Publio R, Roque AC (2013) The periglomerular cell of the olfactory bulb and its role in controlling mitral cell spiking: a computational model. PLoS One 8:e56148.

Assisi C, Stopfer M, Laurent G, Bazhenov M (2007) Adaptive regulation of sparseness by feedforward inhibition. Nat Neurosci 10:1176–1184.

Aston-Jones G, Cohen JD (2005) An integrative theory of locus coeruleus-norepinephrine function: adaptive gain and optimal performance. Annu Rev Neurosci 28:403–450.

Berridge CW, Schmeichel BE, España RA (2012) Noradrenergic modulation of wakefulness/arousal. Sleep Med Rev 16:197–187.

Bouret S, Sara SJ (2005) Network reset: a simplified overarching theory of locus coeruleus noradrenaline function. Trends Neurosci 28:574–582.

Bozza T, McGann JPJP, Mombaerts P, Wachowiak M (2004) In vivo imaging of neuronal activity by targeted expression of a genetically encoded probe in the mouse. Neuron 42:9–21.

Brennan PA, Schellinck HM, de la Riva C, Kendrick KM, Keverne EB (1998) Changes in neurotransmitter release in the main olfactory bulb following an olfactory conditioning procedure in mice. Neuroscience 87:583–590.

Brennan PAA, Keverne EB (1997) Neural mechanisms of mammalian olfactory learning. Prog Neurobiol 51:457–481.

Carcea I, Froemke RC (2013) Cortical plasticity, excitatory-inhibitory balance, and sensory perception. Prog Brain Res 207:65–90.

Chen WR, Shepherd GM (2005) The olfactory glomerulus: a cortical module with specific functions. J Neurocytol 34:353–360.

Ciombor KJ, Ennis M, Shipley MT (1999) Norepinephrine increases rat mitral cell excitatory responses to weak olfactory nerve input via alpha-1 receptors in vitro. Neuroscience 90:595–606.

Day HE., Campeau S, Watson SJ, Akil H (1997) Distribution of α1a-, α1b- and α1d-adrenergic receptor mRNA in the rat brain and spinal cord. J Chem Neuroanat 13:115–139.

Devore S, Linster C (2012) Noradrenergic and cholinergic modulation of olfactory bulb sensory processing. Front Behav Neurosci 6:52.

Fletcher ML, Masurkar A V, Xing J, Imamura F, Xiong W, Nagayama S, Mutoh H, Greer CA, Knöpfel T, Chen WR (2009) Optical imaging of postsynaptic odor representation in the glomerular layer of the mouse olfactory bulb. J Neurophysiol 102:817–830.

Gire DH, Schoppa NE (2008) Long-term enhancement of synchronized oscillations by adrenergic receptor activation in the olfactory bulb. J Neurophysiol 99:2021–2025.

Guérin D, Peace ST, Didier A, Linster C, Cleland TA (2008) Noradrenergic neuromodulation in the olfactory bulb modulates odor habituation and spontaneous discrimination. Behav Neurosci 122:816–826.

Hayar A, Heyward PM, Heinbockel T, Shipley MT, Ennis M (2001) Direct Excitation of Mitral Cells Via Activation of alpha 1-Noradrenergic Receptors in Rat Olfactory Bulb Slices. J Neurophysiol 86:2173–2182.

He J, Ma LM, Kim S, Nakai J, Yu CR (2008) Encoding gender and individual information in the mouse vomeronasal organ. Science (80-) 320:535–538.

Horn G (1986) Memory, Imprinting and the Brain: An Inquiry into Mechanisms (Oxford Psychology Series). Oxford University Press, USA.

Isaacson JS, Strowbridge BW (1998) Olfactory Reciprocal Synapses: Dendritic Signaling in the CNS. Neuron 20:749–761.

Jahr CE, Nicoll RA (1980) Dendrodendritic inhibition: demonstration with intracellular recording. Science (80-) 207:1473–1475.

Jiang M, Griff ER, Ennis M, Zimmer LA, Shipley MT (1996) Activation of locus coeruleus enhances the responses of olfactory bulb mitral cells to weak olfactory nerve input. J Neurosci 16:6319–6329.

Kass MD, Rosenthal MC, Pottackal J, McGann JP (2013) Fear learning enhances neural responses to threat-predictive sensory stimuli. Science 342:1389–1392.

Kendrick KM, Levy F, Keverne EB (1992) Changes in the sensory processing of olfactory signals induced by birth in sheep. Science (80-) 256:833–836.

Kendrick KM, Lévy F, Keverne EB (1991) Importance of vaginocervical stimulation for the formation of maternal bonding in primiparous and multiparous parturient ewes. Physiol Behav 50:595–600.

King PD, Zylberberg J, DeWeese MR (2013) Inhibitory interneurons decorrelate excitatory cells to drive sparse code formation in a spiking model of V1. J Neurosci 33:5475–5485.

Koulakov AA, Rinberg D (2011) Sparse incomplete representations: a potential role of olfactory granule cells. Neuron 72:124–136.

Lin DY, Shea SD, Katz LC (2006) Representation of natural stimuli in the rodent main olfactory bulb. Neuron 50:937–949.

Linster C, Nai Q, Ennis M (2011) Non-linear effects of noradrenergic modulation of olfactory bulb function in adult rodents. J Neurophysiol 105:1432–1443.

Ma L, Qiu Q, Gradwohl S, Scott A, Yu EQ, Alexander R, Wiegraebe W, Yu CR (2012) Distributed representation of chemical features and tunotopic organization of glomeruli in the mouse olfactory bulb. Proc Natl Acad Sci U S A 109:5481–5486.

Mandairon N, Peace S, Karnow A, Kim J, Ennis M, Linster C (2008) Noradrenergic modulation in the olfactory bulb influences spontaneous and reward-motivated discrimination, but not the formation of habituation memory. Eur J Neurosci 27:1210–1219.

McLean JH, Shipley MT, Nickell WT, Aston-Jones G, Reyher CK (1989) Chemoanatomical organization of the noradrenergic input from locus coeruleus to the olfactory bulb of the adult rat. J Comp Neurol 285:339–349.

Meister M, Bonhoeffer T (2001) Tuning and topography in an odor map on the rat olfactory bulb. J Neurosci 21:1351–1360.

Mombaerts P (2006) Axonal wiring in the mouse olfactory system. Annu Rev Cell Dev Biol 22:713–737.

Murphy GJ, Darcy DP, Isaacson JS (2005) Intraglomerular inhibition: signaling mechanisms of an olfactory microcircuit. Nat Neurosci 8:354–364.

Nai Q, Dong H-W, Hayar A, Linster C, Ennis M (2009) Noradrenergic regulation of GABAergic inhibition of main olfactory bulb mitral cells varies as a function of concentration and receptor subtype. J Neurophysiol 101:2472–2484.

Nai Q, Dong HW, Linster C, Ennis M (2010) Activation of alpha1 and alpha2 noradrenergic receptors exert opposing effects on excitability of main olfactory bulb granule cells. Neuroscience 169:882–892.

Olshausen BA, Field DJ (2004) Sparse coding of sensory inputs. Curr Opin Neurobiol 14:481–487.

Pandipati S, Gire DH, Schoppa NE (2010) Adrenergic receptor-mediated disinhibition of mitral cells triggers long-term enhancement of synchronized oscillations in the olfactory bulb. J Neurophysiol 104:665–674.

Petzold GC, Albeanu DF, Sato TF, Murthy VN (2008) Coupling of neural activity to blood flow in olfactory glomeruli is mediated by astrocytic pathways. Neuron 58:897–910.

Pissonnier D, Thiery JC, Fabre-Nys C, Poindron P, Keverne EB (1985) The importance of olfactory bulb noradrenalin for maternal recognition in sheep. Physiol Behav 35:361–363.

Rangel S, Leon M (1995) Early odor preference training increases olfactory bulb norepinephrine. Brain Res Dev Brain Res 85:187–191.

Rubin BD, Katz LC (1999) Optical imaging of odorant representations in the mammalian olfactory bulb. Neuron 23:499–511.

Sachdev RNS, Krause MR, Mazer JA (2012) Surround suppression and sparse coding in visual and barrel cortices. Front Neural Circuits 6:43.

Schoppa NE, Urban NN (2003) Dendritic processing within olfactory bulb circuits. Trends Neurosci 26:501–506.

Shea SD, Katz LC, Mooney R (2008) Noradrenergic induction of odor-specific neural habituation and olfactory memories. J Neurosci 28:10711–10719.

Smith TC, Jahr CE (2002) Self-inhibition of olfactory bulb neurons. Nat Neurosci 5:760–766.

Sullivan R, Stackenwalt G, Nasr F, Wilson D (2000) activation of olfactory bulb noradrenergic β-receptors or locus coeruleus stimulation is sufficient to produce learned approach responses to that odor in neonatal rats. Behav … 114:957–962.

Sullivan RM, Wilson DA, Leon M (1989) Norepinephrine and learning-induced plasticity in infant rat olfactory system. J Neurosci 9:3998–4006.

Sullivan RM, Zyzak DR, Skierkowski P, Wilson DA (1992) The role of olfactory bulb norepinephrine in early olfactory learning. Brain Res Dev Brain Res 70:279–282.

Uchida N, Takahashi YK, Tanifuji M, Mori K (2000) Odor maps in the mammalian olfactory bulb: domain organization and odorant structural features. Nat Neurosci 3:1035–1043.

Usher M, Cohen J, Servan-Schreiber D, Aston-Jones G (1999) The role of locus coeruleus in the regulation of cognitive performance. Science (80-) 283:549–554.

Valentino RJ, Van Bockstaele E (2008) Convergent regulation of locus coeruleus activity as an adaptive response to stress. Eur J Pharmacol 583:194–203.

Wachowiak M, Cohen LB (2001) Representation of odorants by receptor neuron input to the mouse olfactory bulb. Neuron 32:723–735.

Wilson DA, Sullivan RM, Leon M (1987) Single-unit analysis of postnatal olfactory learning: modified olfactory bulb output response patterns to learned attractive odors. J Neurosci 7:3154–3162.

Winzer-Serhan U., Raymon H., Broide R., Chen Y, Leslie F. (1996) Expression of α2 adrenoceptors during rat brain development—II. α2C messenger RNA expression and [3H]rauwolscine binding. Neuroscience 76:261–272.

Winzer-Serhan UH, Raymon HK, Broide RS, Chen Y, Leslie FM (1997) Expression of α2 adrenoceptors during rat brain development—I. α2A messenger RNA expression. Neuroscience 76:241–260.

Yu CR, Power J, Barnea G, O'Donnell S, Brown HEV, Osborne J, Axel R, Gogos JA (2004) Spontaneous neural activity is required for the establishment and maintenance of the olfactory sensory map. Neuron 42:553–566.

Yuan Q, Harley CW, McLean JH, Knopfel T (2002) Optical imaging of odor preference memory in the rat olfactory bulb. J Neurophysiol 87:3156–3159.